J Mater Sci (2009) 44:2257–2263
DOI 10.1007/s10853-008-3146-4

FESTSCHRIFT IN HONOUR OF PROF T R ANANTHARAMAN ON THE OCCASION OF HIS 80TH BIRTHDAY

The effect of ball milling on the melting behavior of Sn–Cu–Ag eutectic alloy

Bhupal Reddy · P. Bhattacharya · Bawa Singh · K. Chattopadhyay

Received: 29 June 2008 / Accepted: 1 December 2008 / Published online: 31 December 2008

Abstract Sn–Ag–Cu (SAC) solder alloys are the best Pb free alternative for electronic industry. Since their introduction, efforts are made to improve their efficacies by tuning the processing and composition to achieve lower melting point and better wettability. Nanostructured alloys with large boundary content are known to depress the melting points of metals and alloys. In this article we explore this possibility by processing prealloyed SAC alloys close to SAC305 composition (Sn-3wt%Ag-0.5wt%Cu) by mechanical milling which results in the formation of nanostructured alloys. Pulverisette ball mill (P7) and Vibratory ball mills are used to carry out the milling of the powders at room temperature and at lower temperatures (−104 °C), respectively. We report a relatively smaller depression of melting point ranging up to 5 °C with respect to original alloys. The minimum grain sizes achieved and the depression of melting point are similar for both room temperature and low-temperature processed samples. An attempt has been made to rationalize the observations in terms of the basic processes occurring during the milling.

B. Reddy · P. Bhattacharya (✉) · K. Chattopadhyay
Department of Materials Engineering, Indian Institute of Science, Bangalore 560 012, India
e-mail: prajina.bhattacharya@ge.com

B. Singh
Cookson Electronics Assembly Materials, 600 Route 440, Jersey City, NJ 07304, USA

Introduction

Sn–Pb solder has been the prevalent material for interconnects and packaging of modern electronic components and devices. The widespread use of Sn–Pb solders is primarily due to their cost and convenient material properties like low melting temperature, good wettability, etc. However, Pb and Pb-containing products are highly toxic which poses threat to human beings. In view of environmental and health concerns, substantial effort is being made to develop Pb-free solders as replacement of conventional Sn–Pb solders. For a variety of reasons, Sn–Ag–Cu (SAC) ternary alloy has been the most successful material as a replacement of Sn–Pb solders.

One of the major drawbacks of lead free solders containing silver is their relatively high melting temperature compared to eutectic Sn–Pb, the other disadvantage commercially being that Ag is expensive.

It is well known that reduction of grain size can lead to the reduction of melting point as the excess energy stored in the grain boundaries as well as the capillarity reduces the total enthalpy of melting [1]. With the current emphasis on nanoscience, the melting transition of materials with reduced microstructural length scale has been explored extensively [2]. It is shown that the nature of the interface plays a major role in altering the melting points of metals and alloys. If the interface constraints the Debye Waller vibration, one may even expect superheating [3, 4]. However, in general, for a disordered interface, a depression of melting point is promoted. Thus the microstructure modifications leading to nanostructured materials represent a good alternative for the reduction of the melting point.

Alloying additions of low melting point elements like Bi provides one of the possibilities for the reduction of the melting points. Bi addition, however, may enhance the

undesirable problem of fillet lifting/tombstoning in soldering applications especially in the SAC system [5, 6].

One of the exciting process developments in recent time is the discovery of the possibility of the large reduction of the grain size by severe plastic deformation [7]. Mechanical milling is one of the most widespread techniques to impart such high rate of mechanical energy input [8]. In this process mechanical mixing also occurs due to large plastic flow as well as repeated fracturing and welding during milling. It is increasingly realized that the process of evolution of nanograins represents optimization between processes that promote smaller grains (with increased stored energy) and the process, which promote relaxation and grain growth. Experimental results repeatedly point to a limit of achievable grain size which depends on melting point, modulus, the rate of strain hardening as well as diffusivity and kinetics of grain growth [9]. These are, in most cases, dependent on the intrinsic properties of materials. Thus different materials are expected to exhibit different limits for achievable grain size.

Melting point depression of nanostructured materials is of potential interest for electronic packaging. It is particularly relevant for lead free tin-based solders. These Pb free Sn based typically have higher melting point than the Sn–Pb solders of earlier generation. There are past efforts in developing lead free solders by mechanical alloying route. Huang et al. [10] prepared Sn–Zn and Sn–Sb solder alloy by mechanical alloying directly from the elemental powders. Lai and Duh [11] have synthesized Sn–Ag and Sn–Ag–Bi solder alloys by mechanical alloying and reported a better wettability. Duh and co-workers [12, 13] explored different compositions of the SAC and Sn–Ag–Ni lead free solders and the composite containing Cu_6Sn_5 and Ni_4Sn_3 nanoparticles by mechanical alloying. Surprisingly, these researchers have reported a retardation of the formation of the intermetallic phases at the interfaces in the milled samples [14].

The present work deals with the SAC system. In the Sn rich side two intermetallic phases has been reported in this system, namely, Ag_3Sn and Cu_6Sn_5. Both these phases form eutectics in binary Ag–Sn and Cu–Sn systems with eutectic compositions being 3.5 wt% Ag and 0.7 wt% Cu, respectively. The corresponding eutectic temperatures are 221 °C and 227 °C, respectively. The melting range of ternary alloys is between 217 and 220 °C for alloys containing Ag in the range of 3–4 wt% and Cu 0.5–1.0 wt%. Sn has tetragonal structure at room temperature with Space Group $I4_1/amd$, with $a = 0.583$ nm, $c = 0.319$ nm while Ag_3Sn is orthorhombic with Space Group Pmmn, $a = 0.557$ nm, $b = 0.478$ nm, $c = 0.518$ nm and Cu_6Sn_5 is monoclinic with Space Group C2/c, $a = 1.103$ nm, $b = 0.729$ nm, $c = 0.983$ nm and $\beta = 98.82$. Sn also undergoes a transformation at 13.2 °C and the structure is cubic with Space Group $Fd\bar{3}m$, $a = 0.649$ nm.

The aim of the present investigation is to investigate the possibility of the reduction of the melting point of the SAC lead free solders by producing nanostructured alloys through mechanical alloying and explore the limit of the grain size that is achievable in these alloys under different conditions of milling including cryomilling.

Experimental

Type III (25–40 μm) SAC305 (Sn3wt%Ag0.5wt%Cu) powder was used in the present investigation. This is a commercial alloy supplied by Woking, England. The average particle size was measured to be 35 μm using laser particle analyzer. The milling has been carried out in two different mills. First one is Pulverisette ball mill (P7) in which the cylindrical vials (2 numbers) and supporting disk rotates in opposite directions. Milling was carried out at room temperature under toluene to prevent oxidation and cold-welding of the powder particles. Ball-to-powder ratio (BPR) was maintained at 8:1. 250 ml capacity WC vials and WC balls (3 numbers) were used. Milling was carried out at different rotational speeds of the vials at intensity settings of 5 (400 rpm) and 8 (580 rpm). Around 0.5 g of sample was collected at regular intervals of 5 h for characterization studies and milling was continued till 25 h. As a result of the sample withdrawal, there is a slight increase in the ball to powder ratio with time. However, the effect of such increase has been ignored in this article.

Milling was also carried out in Fritsch Analysette 3 Spartan Pulverisette cryomill, which operates on the principle of vibration in the vertical direction. The milling was carried out with only one WC ball (0.5 kg) in a WC vial. Cyclohexene was poured around the vial and was frozen by using liquid nitrogen. Hence the temperature was maintained at around −104 °C, which is the freezing point of cyclohexene. BPR was taken as 25:1. A small amount of toluene was added in this set up as well to prevent excessive cold welding of the particles.

The preliminary detection of phases was done through X-ray diffraction. A JEOL X-ray diffractometer JDX 8080 was used with a copper K_α radiation. In all cases precision lattice parameters were determined by '$\cos\theta\ \cot\theta$' extrapolation after correcting for instrumental broadening using Si standard. The effect of grain size and strain were determined by Scherrer–Wilson method with the peak shape approximated by the Cauchy–Gaussian relationship. A JEOL JSM 840A Scanning Electron Microscopy (SEM) was used to observe the surface microstructure of the powders and their surface morphologies. Energy Dispersive Spectroscopy (EDS), which is attached with SEM, was carried out to find out the composition and contamination, if any, of the milled powders.

Differential Scanning Calorimeter (DSC) experiments were carried out using a Mettler Toledo calorimeter to extract the enthalpy values and melting temperatures of the milled powders. A cooling rate of 10 °C was used for all the measurement. For the measurement of enthalpy, the instrument was calibrated using the melting transition of high purity indium. The onset of the peak was used as a measure of melting temperature. The undercoolings achieved in processed alloys were measured with respect to the melting of the bulk alloy.

Results

Sn–Ag–Cu (SAC) powder: P7(int-5); RT milling

The X-ray diffraction patterns for different milling times are shown in Fig. 1a and the relevant phases for the corresponding Bragg reflections are indicated on the plot. The patterns exhibit well-defined Sn peaks of tetragonal structure and weak reflections from Ag_3Sn. It can be observed that the peaks were broadened with continued milling, suggesting a grain refinement process of the powder particles and development of lattice strain. No reflection could be matched with oxides of Sn, Ag, and Cu. Weak reflections of Tungsten Carbide (WC) can also be seen, which indicates a possible contamination of the powder with the WC (~5 at%) during milling. Lattice parameter measurements for Sn-rich phase with milling time are shown in the Fig. 1b. No change of lattice parameter in both 'a' and 'c' with milling time could be detected.

Scherrer–Wilson equation with Cauchy–Gauss peak fitting was used to calculate the average crystallite size of the Sn-rich and Ag_3Sn phases for different milling times and the results are shown in Fig. 1c. It can be seen that the

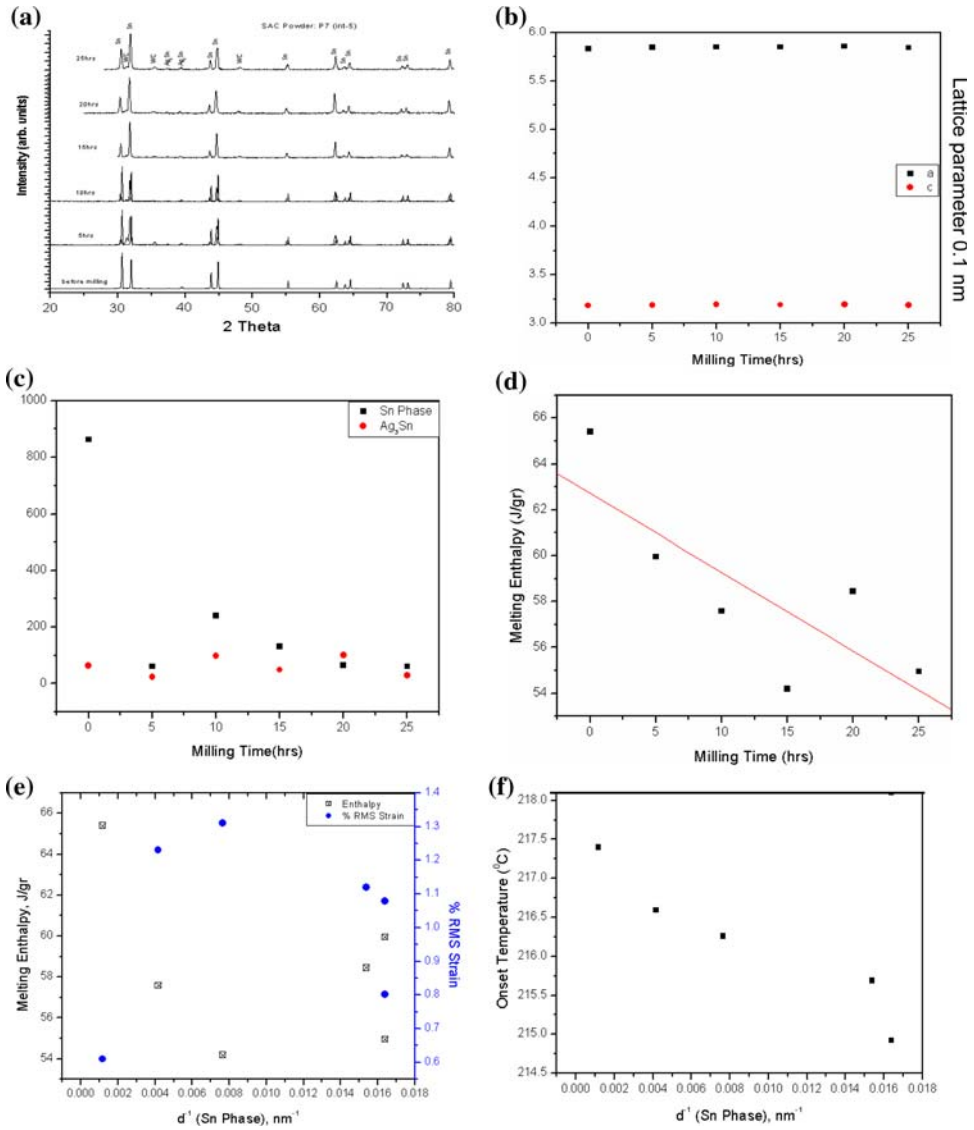

Fig. 1 The P7 ball milled powder with intensity 5 shows **a** X-Ray diffraction patterns, **b** variation of crystallite size, **c** lattice parameters both 'a' and 'c', **d** melting enthalpies with milling time, **e** effect of crystallite size on melting enthalpy and lattice strains, and **f** onset temperature milling time

crystallite size of the Sn-rich phase reduces at a faster rate to <60 nm in the early stages of the milling. With continued milling, crystallite size reduces at slower rate and reaches a steady state. However, the crystallite size of the Ag_3Sn remains unchanged. The rms strain measurements are derived from the slope of the Scherrer–Wilson plots. Two regions can be distinguished: in the first region the lattice strain increases and reaches a maximum value while in the second region lattice strain decreases. As crystallite size decreases the lattice strain increases, reaches a maximum followed by a reduction. Melting enthalpy, as measured by the calorimeter, also decreases with milling time (Fig. 1d). Thus, enthalpy associated with the melting of the powder particles decreases with crystallite size. In Fig. 1e we have plotted both the rms strain and melting enthalpy as a function of the inverse of the grain size. This indicates that the stored enthalpy (energy) increases with milling time. The decrease of the onset temperature of melting of the powder can be observed (Fig. 1f) with continued milling. The onset temperature is observed to decrease to around 214.5 °C after 25 h of milling.

Sn–Ag–Cu (SAC) powder: P7(int-8); RT milling

X-ray diffraction patterns of the powder samples milled with intensity 8 (580 rpm) show very similar results. The milled powders again exhibit Sn and Ag_3Sn reflections. The broadening of the peaks could be observed with the milling time. No peaks could be matched with oxides of Sn, Ag, or Cu. A small amount of contamination ($\sim$3 at %) with tungsten carbide could be observed from EDS experiments. There is no change in lattice parameters 'a' and 'c' of Sn-rich phase. The average crystallite sizes were calculated from Scherrer's formula and the variation of the average crystallite size with milling time is shown in Fig. 2a.

It can be seen in this case as well that the crystallite size of Sn-rich phase reduces at faster rate in the early stages of the milling followed by slow rate of reduction and reaches a steady state after $\sim$15 h of milling with size $\sim$100 nm. The crystallite size of Ag_3Sn was observed to achieve a steady state around $\sim$45 nm. The melting enthalpy decreases with the milling time. The effect of crystallite size on lattice strain and enthalpy is shown in Fig. 2b. The lattice strain exhibits two regions, in which strain increases and reaches a maximum in the first region followed by a decrease. It can be seen (Fig. 2c) that the onset temperature is decreased to around 212 °C.

Direct cryomilling of SAC powder

Direct cryomilling of the SAC powders result in reduction of grain size of both Sn and Ag_3Sn phases (Fig. 3a). The crystallite size of the Sn-rich phase reduces at a faster rate,

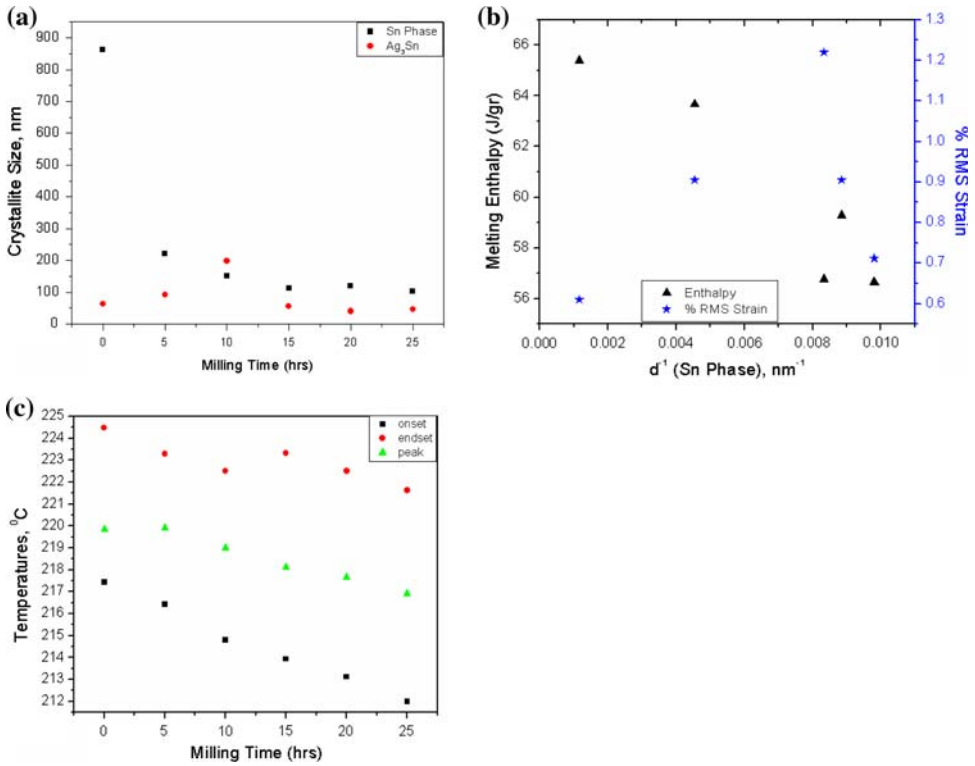

Fig. 2 The P7 ball milled powder with intensity 8 shows **a** variation of crystallite size, **b** effect of crystallite size on melting enthalpy and lattice strains, and **c** onset, peak, and end of melting temperatures with milling time

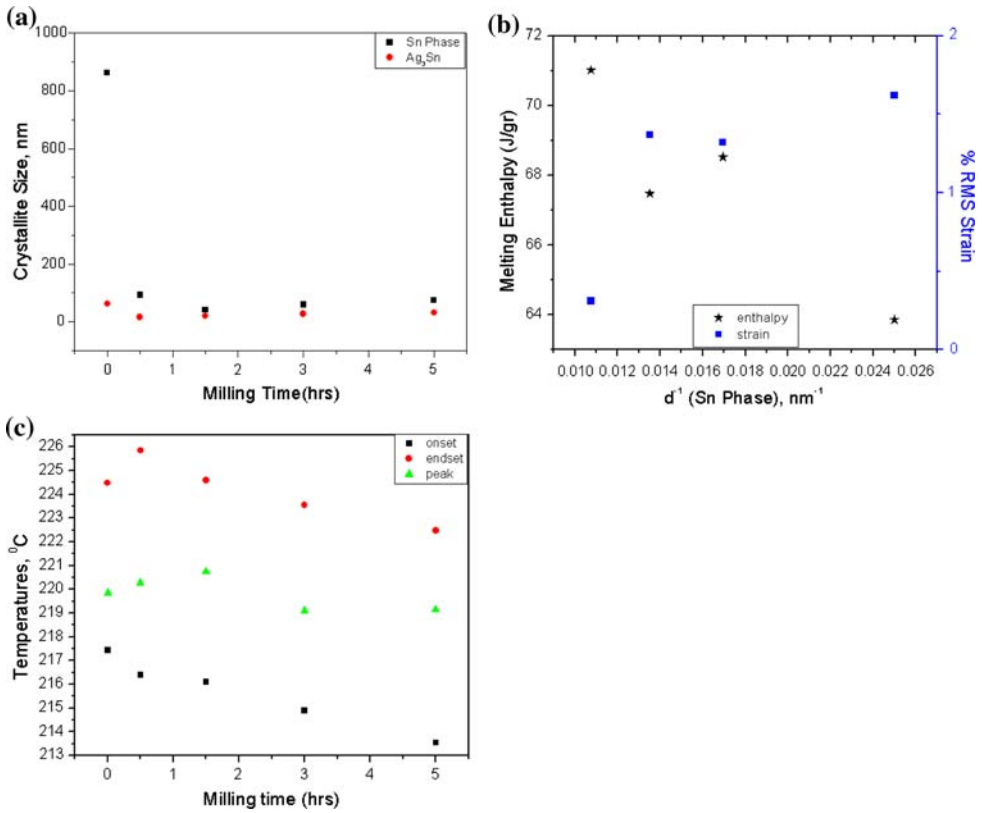

Fig. 3 The cryomilled powder samples show **a** variation of crystallite size with milling, **b** effect of crystallite size on melting enthalpy and lattice strains, and **c** onset, peak, and end of melting temperatures with milling time

to <100 nm. The grain size obtained a minimum at 1.5 h of milling followed by a slight increase particularly for Sn-rich phase. However, there is no change in the lattice parameters, both in 'a' and 'c'.

The lattice strain decreases at the early stages of milling and subsequently exhibits an oscillatory behavior. The melting enthalpy on the other hand decreases with the reduction of crystallite size. This is shown in Fig. 3b. The increase in strain is around 1.8% (Fig. 3b), which is more than the values of strains measured for room temperature milling (~1.3%). The onset temperature for melting is observed to decrease continuously with the milling time. The onset temperature is around 213.5 °C after 5 h of milling (Fig. 3c). Some of the salient results of the cryomilling are summarized in Table 1.

Table 1 Summary of the results of the cryomilled alloys obtained in the present investigation

Milling time (h)	Crystallite size (nm)		$T_{(onset)}$ (°C)
	Sn-phase	Ag_3Sn	
0	672	63	217.4
0.5	22	16	216.4
1.5	40	21	216.1
3.0	59	27	214.9
5.0	74	31	213.5

Discussions

We first summarize the main experimental results of the present study. The refined grain size, that can be achieved by milling the Sn3wt%Ag0.5wt%Cu alloy powders at room temperature, is of the order of 100 nm for Sn-rich phase. The ultimate reduction of size does not depend on the intensity of milling. However, it affects the rate of reduction. The rate of reduction of grain size is very rapid during cryomilling. However, grain sizes observed in our experiments after cryomilling indicates a grain growth at later stages for the Sn rich. The d_{min} obtained via cryomilling in the present case is not very different from that obtained by room temperature milling (100 nm versus 75 nm for the Sn-rich phase). Similar results were observed earlier in the case of Al [15].

This is also reflected in the depression of the melting point. While the melting point depression of the alloy for low intensity milling is 2.5°, it is ~5 for the high intensity milling and 3.5° for cryomilling. The accumulated strain (% rms strain obtained from line broadening) shows a peak as a function of milling for room temperature samples

indicating a process of recovery setting in during prolonged milling. In contrast, in our cryomilling experiments high rms strain was retained since recovery being thermally assisted process was sluggish.

The minimum achievable grain size during mechanical milling has been subject of several investigations. The work on pure metals has been summarized by Koch [7] who has shown that there exists an inverse relation between achievable grain size and melting temperature. For alloys, however, different hardening mechanism operates including nucleation of grains in the shear bands as well as recovery process and grain rotation [15, 16]. Recently Mohamed [9] has developed a detailed model for evolution of grain size during mechanical milling of metals and alloys. Mohamed's model [9] invokes equations that describe the balance between strain hardening by dislocation generation and thermal recovery leading to dislocation annihilation. This dislocation model shows that if the temperature effect on shear modulus is ignored, minimum grain size that can be obtained is written as:

$$d_{min} = A[(e^{\frac{-\beta Q}{4RT}})/(T)^{0.25}$$

where A is constant, d_{min} is the minimum grain size, βQ is the activation energy for recovery process, R is the universal gas constant, T is the temperature of operation in K.

The model relates the dependence of d_{min} on hardness, stacking fault energy and activation energy for recovery. As the exponential term dominates, smaller grain size is expected at lower milling temperatures while the lower hardness of our alloy should give a bigger size.

Both for room temperature and cryomilling, the grain size reduction is very rapid in the early stages. There can be two different possibilities to explain this result. Repeated welding followed by fracturing can cause decrease in the grain size rapidly. On the other hand some investigators invoked shear banding and dynamic recrystallisation at the shear bands for the rapid decrease in grain size especially for low temperature milling. Since the melting point of the alloy is low ($\sim$221 °C), both the mechanisms could be operative at room temperature as T/T_m is $\sim$0.4. The rapid reduction in grain size during cryomilling could be because of the increased strain hardening rate at lower temperature of −104 °C. Severe deformation during cryomilling could initially form small angle grain boundary followed by grain rotation [17]. Further reduction is slow probably due to approach of a balance between strain hardening and progress in dynamic recrystallization.

Root mean square strain in all samples milled under three different conditions exhibit increasing trend with milling time. The magnitude of strain is similar for both the cases of milling at intensities 5 and 8 in P7 ball mill (1.3 and 1.28%, respectively) at room temperature. In cryomilling, lattice strain values are higher (around 1.8%). Our results are consistent with the reported work of Zhang et al. [18].

The melting enthalpy in all these cases decrease with milling time indicating accumulation of stored energy. However, when plotted against inverse of the grain size, one observes fluctuations at higher milling time indicating the setting in of the recovery process. In contrast cryomilled samples show a decreasing trend indicating continuing increase in the stored energy. Thus, the recovery process is sluggish at the low temperature of milling. The observation of melting enthalpy compliments our previous observation of strain accumulation.

Melting temperature is observed to decrease by 2.5 and 5 °C for room temperature milling carried out at P7 with intensity 5 and 8 for 25 h. In the case of cryomilling 3.5 °C reduction in melting point is observed after 5 h of milling. Thus cryomilling in this system does not provide any additional advantage of meeting the target of reducing melting temperature.

Lack of large depression of melting point observed during cryomilling need rationalization. The observed behavior which indicates grain sizes of cryomilled samples of the same orders as that of room temperature milled samples is most likely the results of more than one competing mechanism. We note that the actual measurement of the grain size was carried out only at room temperature in all cases. The cryomilling in general is expected to lead to a more efficient reduction of grain size as the process of fracturing is easier at lower temperature. However, in the case of alloys primarily consisting of Sn the comparison of room temperature milling and cryomilling is not straightforward. Sn undergoes allotropic transformation from white Sn (body centered tetragonal) to gray tin (diamond cubic) at 13.2 °C. Although this transformation requires large incubation period, it can be enhanced by cold deformation [19, 20]. Thus the observed structure at room temperature may also be influenced by the reverse transformation and associated recovery processes.

The WC contamination is observed to be lower ($\sim$3 at.%) for high intensity milling (Intensity 8) as compared to 5 at. % obtained for powders milled at lower intensity (Intensity 5) at room temperature. Our hypothesis is that the impact component could be more at high rpm that results in less contamination compared to grinding action of the ball that dominates at low speeds. However, this needs to be proven.

Conclusions

In all cases of milling (room temperature and cryomilling), crystallite size reduces rapidly to <100 nm, which is attributed to the dynamic recrystallisation of the Sn-rich

phase, as its recrystallisation temperature is 4 °C. A depression of melting temperature of 2.5 °C, and 5 °C could be achieved in the case of P7 milling with intensities 5 and 8, respectively, after 25 h of milling. In the case of cryomilling the depression is 3.5 °C—suggesting accrual of no advantage. The depression of melting temperature, which is not very large, can be attributed to the enhanced strain energy associated with the imperfections and decrease in grain size. Thus significant depression in melting or grain size reduction could not be achieved in these systems even after cryomilling.

References

1. Ehrhardt H, Weissmuller J, Wilde G (2001) Mater Res Soc Symp Proc B8.6.1:634
2. Chattopadhyay K, Goswami R (1997) Prog Mater Sci 42:287
3. Goswami R, Chattopadhyay K (1993) Phil Mag Lett 68:215
4. Goswami R, Chattopadhyay K (1995) Acta Metal Mater 43:2837
5. Hwang JS (2001) Environment friendly electronics: lead free technology. Electrochemical Publications, IOM, Great Britain
6. Hwang JS (1994) In: Proceedings, surface mount international, p 405
7. Koch CC (1997) Nanostruct Mater 9:13
8. Suryanarayana C (2005) Mechanical alloying and milling. Taylor and Francis Group, Oxford
9. Mohamed FA (2003) Acta Mater 51:4107
10. Huang ML, Wu CML, Lai JKL, Wang FG (2000) J Mater Sci Mater Electron 11:57
11. Lai HL, Duh JG (2003) J Electron Mater 32:215
12. Kao ST, Duh JG (2004) J Electron Mater 33:1445
13. Lee HY, Duh JG (2006) J Electron Mater 35:494
14. Kao ST, Lin YC, Duh JG (2006) J Electron Mater 35:486
15. Fecht HJ (1995) Nanostruct Mater 6:33
16. Shen TD, Koch C (1996) Acta Mater 44:753
17. Witkin DB, Lavernia EJ (2006) Prog Mater Sci 51:1
18. Zhang X, Wang H, Narayan J, Koch CC (2001) Acta Mater 49:1319
19. Joo YJ, Takemoto T (2002) Mater Lett 56:793
20. Burgers WG, Groen LJ (1957) Dicuss Faraday Soc 23:183